ELSEVIER

Journal of Power Sources 113 (2003) 11–18

JOURNAL OF POWER SOURCES

www.elsevier.com/locate/jpowsour

Effect of channel dimensions and shape in the flow-field distributor on the performance of polymer electrolyte membrane fuel cells

Atul Kumar, Ramana G. Reddy*

Department of Metallurgical and Materials Engineering, The University of Alabama, A129 Bevill Building Box 870202, Tuscaloosa, AL 35487 0202, USA

Received 14 August 2002; accepted 31 August 2002

Abstract

This work concentrates on the improvement in the performance of the polymer electrolyte membrane fuel cell (PEMFC) through optimization of the channel dimensions and shape in the flow-field of bipolar/end plates. Single-path serpentine flow-field design was used for studying the effect of channel dimensions on the hydrogen consumption at the anode. Simulations were done ranging from 0.5 to 4 mm for different channel width, land width and channel depth. Optimum values for each of the dimensions (channel width, land width and channel depth) were obtained. For high hydrogen consumptions (~80%), the optimum dimension value for channel width, land width and channel depth was close to 1.5, 0.5 and 1.5 mm, respectively. Studies on the effect of channel shapes showed that triangular and hemispherical shaped cross-section resulted in increase in hydrogen consumption by around 9% at the anode. Consequently, their use would lead to improved fuel cell efficiency.

Keywords: Fuel cells; PEMFC; Bipolar plate; Flow-field channels; CFD; Fluent

1. Introduction

Fuel cells are electrochemical devices that can efficiently convert the chemical energy (oxidation potential) of the fuel directly into electrical energy. They operate like batteries and are similar in components and characteristics, but unlike batteries, they do not get exhausted and are environmentally friendly. As long as fuel is supplied to the cell along with an oxidant (typically air), the fuel cell continues to produce electrical energy and heat.

The use of fuel cells has several advantages over the conventional power generation systems. They offer a source of electrical energy that is continuous (as long as fuel is provided), environmentally safe and always available. Additional benefits include low maintenance, excellent load performance, etc. In fuel cells, the chemical energy is directly converted into electricity, i.e. without preliminary conversion to heat. Consequently, this conversion is not limited by the Carnot cycle and efficiencies as high as 90% can be obtained.

Several types of fuel cells exist: polymer electrolyte membrane fuel cell (PEMFC), alkaline fuel cell, phosphoric fuel cell, molten carbonate fuel cell, solid oxide fuel cell, which are in different stages of development [1]. The PEMFC is seen as a system of choice for automotive applications due to several advantages that this fuel cell offers over the other types. PEMFCs operate at low temperatures (~80 °C), allowing for faster startups and immediate response to changes in the power demand. The PEMFC consists of an anode and a cathode with a proton exchange membrane sandwiched in between. Hydrogen is supplied at the anode where it dissociates into charged protons and electrons. The protons migrate across the membrane onto the cathode side while the electrons flow through the outer circuit generating electricity. These protons and electrons combine at the cathode and react with oxygen to produce water. The electrochemical reactions are:

$$\text{anodic}: \quad H_2 \rightarrow 2H^+ + 2e^- \tag{1}$$

$$\text{cathodic}: \quad \tfrac{1}{2}O_2 + 2H^+ + 2e^- \rightarrow H_2O \tag{2}$$

$$\text{net reaction}: \quad H_2 + \tfrac{1}{2}O_2 \rightarrow H_2O \tag{3}$$

Fuel cell vehicles (FCVs) termed as zero emission vehicles (ZEVs) of the future are one option to meet new and

* Corresponding author. Tel.: +1-205-348-1740; fax: +1-205-348-2164.
E-mail address: rreddy@coe.eng.ua.edu (R.G. Reddy).

0378-7753/02/$ – see front matter © 2002 Elsevier Science B.V. All rights reserved.
PII: S0378-7753(02)00475-5

stringent EPA emission standards. Despite significant technological progress by Partnership for a New Generation of Vehicles (PNGV) in making fuel efficient vehicles, the production models slated for debut in 2004 will not meet EPA emission standards [2]. Fuel cell vehicles have the greatest potential to meet these standards and fuel-efficiency requirements. The focus is now on mass production and commercialization of hydrogen powered FCVs.

However, some technical issues still exist that prohibit the commercialization of these types of fuel cells. These are: (1) electrocatalyst poisoning by low-level carbon monoxide concentration in the fuel; (2) water management and membrane operating temperature limits; (3) cell life; and (4) fuel cell materials and system operating costs. The biggest challenge for the development of fuel cells for automotive applications is reduction of the cost of the cell stack (currently at $ 500 per kW while the 2004 PNGV goal is $ 50 per kW [3]). The high cost is mainly ascribed to the use of materials such as precious metal catalysts, Nafion® membrane and bipolar/end plates. The stringent requirements in terms of the compactness, high energy density, performance stability and low cost changed the fuel cell research direction to that of optimizing the different aspects of PEMFC system.

The efficiency of the fuel cell depends upon the kinetics of the electrochemical process and performance of the components. Several experiments have been conducted by researchers for varying design dimensions of the cell components, operating parameters, etc. However, experimental investigations are costly and models have been developed to understand and optimize the kinetics of the process. Several models which explain the mass transport effect of different species in the fuel cell are developed and these models can very precisely predict the cell performance. However, little focus is being given on the design dimensions of the fuel cell, typically those of the bipolar/end plate's flow-field. This work therefore concentrates on studying the effect of dimensions and shape of the channels in the flow-field of the bipolar plate. This would help to better understand some of the design considerations for the bipolar plates and give the fuel cell developers a scope of further improvement of the fuel cell technology.

2. Model development

The polymer electrolyte membrane model described here is developed to study the effect of the channel dimensions and shape in the flow-field of the bipolar/end plates. Consequently, to avoid complexities, we decided to develop the half-cell model for the anode side of the fuel cell. The problem domain for the half-cell PEMFC model consists of three different zones, viz. (1) flow-field channels (serpentine design) which are imprinted onto the bipolar plates; (2) gas diffusion electrode; and (3) catalyst layer. It was assumed that fuel was hydrogen on the anode side. The hydrogen gas enters the domain at gas inlet in the bipolar plate. The flow-field in the bipolar plate helps in the distribution of hydrogen reactant gas onto the surface of the electrode. The gas is transported towards the anode electrode via diffusion and convective transfer. The next layer is the catalyst layer, where hydrogen molecule breaks into the protons and the electrons.

We decided to choose the rectangular cross-section channels for studying the effect of channel dimensions. The flow-field was chosen to be single-path serpentine design. Once the optimum channel dimensions have been achieved, we would then compare the results with those for other channel shapes.

2.1. Problem domain

Fig. 1 shows the serpentine flow-field design for the bipolar plate with rectangular cross-section channels, showing typical dimensions for channel width, land width and channel depth. Since we are studying the effect of channel dimensions on the fuel cell performance, we have used many different dimensions for the channels. Each of channel width, land width and channel depth was varied from 0.5 to 4.0 mm. The representation in Fig. 1 is only a typical representation for one of the several cases for the channels dimensions used in simulations. The active area of the domain was 4.0 cm (length) × 4.0 cm (width). The thickness of the gas distribution electrode and catalyst layer was taken to be 0.25 and 0.05 mm, respectively. All these zones were taken for the anode side of the cell only. The cross-section of the problem domain is shown in Fig. 2.

2.2. Model assumptions

The following assumptions were used in developing the half-cell model for studying the effect of channel dimensions on the performance of the fuel cell:

(1) Steady state and stationary conditions exist in the single cell stack. Also, the effect of gravity was neglected.
(2) Isothermal conditions exist in the cell domain.
(3) Based on the Reynolds number calculation the flow in the fuel cell is laminar. Hence, all the transport equations were formulated for laminar behavior.
(4) The permeability of the electrode material is assumed to be isotropic and has a value of 10^{-12} m^2.
(5) The volume of the by-product liquid H_2O was assumed to be negligible in the domain.
(6) Since the density of the reactant gas (H_2) varies from location to location in the domain, compressible gas technique [4] was used to determine the density of the gas mixture.

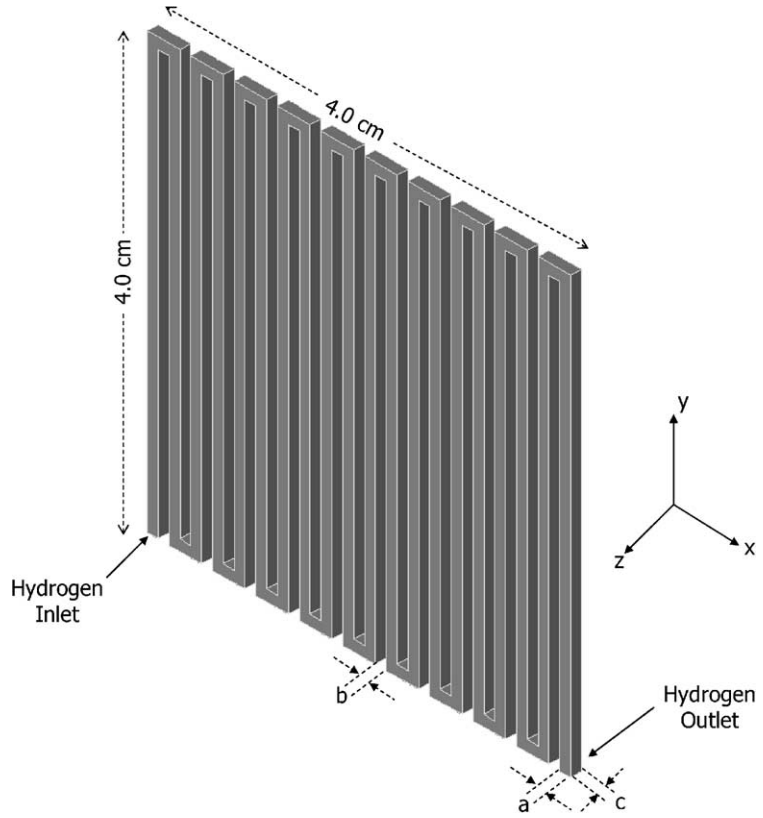

Fig. 1. Serpentine flow-field design in bipolar plate showing typical dimensions for channel width (a), land width (b) and channel depth (c).

2.3. Governing transport equations

The basic transport equations (conservation of mass and momentum) were written for each of the zones of the domain. The conservation of mass, also called equation of continuity is given by:

$$\frac{\partial(\rho v_x)}{\partial x} + \frac{\partial(\rho v_y)}{\partial y} + \frac{\partial(\rho v_z)}{\partial z} = S_m \tag{4}$$

where ρ is the density of the fluid in the medium, and v_x, v_y and v_z are the components of the velocity in x-, y-, and z-direction, respectively. The source term, S_m appears due to the electrochemical reaction and corresponds to the consumption of hydrogen, and is given by [5]:

$$S_m = 0, \quad z_0 \le z \le z_2 \tag{5}$$

$$S_m = -\frac{\lambda[\mathrm{H_2}]}{\kappa + [\mathrm{H_2}]}, \quad z_2 \le z \le z_3 \tag{6}$$

where $[H_2]$ denotes the concentration of hydrogen in the domain, λ and κ are terms that have no physical meaning and their value depends upon the rate constants for the atomic oxidation of H_2 and platinum loading in the catalyst layer. As discussed by Hontanon et al. [5], the value of κ was set equal to 1. Since the value of λ may change from one fuel

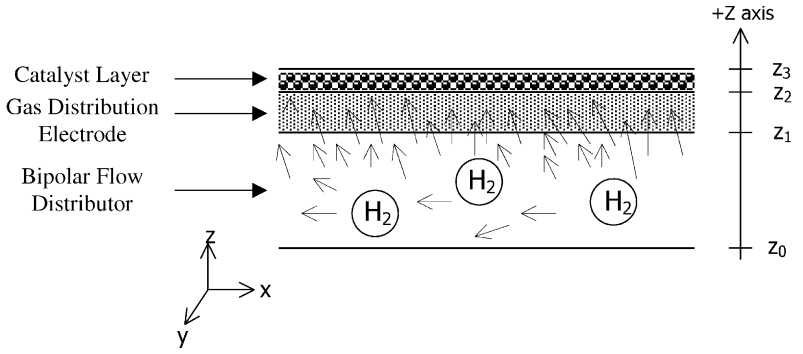

Fig. 2. Half-cell cross-section of the polymer electrolyte membrane fuel cell.

Table 1
Dimensions of different zones and volume mesh element for each zone considered in half-cell model

Zone name	Zone dimensions ($X \times Y \times Z$, mm × mm × mm)	Size of hexahedron volume element ($X \times Y \times Z$, mm × mm × mm)	Total number of volume elements
Flow-field distributor	40 × 40 × c[a]	0.25 × 0.25 × 0.25	6,400 × c
Gas distribution electrode	40 × 40 × 0.25	0.25 × 0.25 × 0.0625	102,400
Catalyst layer	40 × 40 × 0.05	0.25 × 0.25 × 0.05	25,600

[a] c is the channel thickness in the flow-field of bipolar plate and may vary between 0.5 and 4 mm depending on the chosen case.

cell system to another, we will present cases corresponding to different values of λ.

The conservation of momentum, also called as Navier–Stokes equation is given by:

momentum (x-direction):

$$v_x\frac{\partial(\rho v_x)}{\partial x}+v_y\frac{\partial(\rho v_x)}{\partial y}+v_z\frac{\partial(\rho v_x)}{\partial z} = -\frac{\partial P}{\partial x}+\frac{\partial}{\partial x}\left(\mu\frac{\partial v_x}{\partial x}\right)+\frac{\partial}{\partial y}\left(\mu\frac{\partial v_x}{\partial y}\right)+\frac{\partial}{\partial z}\left(\mu\frac{\partial v_x}{\partial z}\right)+S_{px} \quad (7)$$

momentum (y-direction):

$$v_x\frac{\partial(\rho v_y)}{\partial x}+v_y\frac{\partial(\rho v_y)}{\partial y}+v_z\frac{\partial(\rho v_y)}{\partial z} = -\frac{\partial P}{\partial y}+\frac{\partial}{\partial x}\left(\mu\frac{\partial v_y}{\partial x}\right)+\frac{\partial}{\partial y}\left(\mu\frac{\partial v_y}{\partial y}\right)+\frac{\partial}{\partial z}\left(\mu\frac{\partial v_y}{\partial z}\right)+S_{py} \quad (8)$$

momentum (z-direction):

$$v_x\frac{\partial(\rho v_z)}{\partial x}+v_y\frac{\partial(\rho v_z)}{\partial y}+v_z\frac{\partial(\rho v_z)}{\partial z} = -\frac{\partial P}{\partial z}+\frac{\partial}{\partial x}\left(\mu\frac{\partial v_z}{\partial x}\right)+\frac{\partial}{\partial y}\left(\mu\frac{\partial v_z}{\partial y}\right)+\frac{\partial}{\partial z}\left(\mu\frac{\partial v_z}{\partial z}\right)+S_{pz} \quad (9)$$

The source terms in the above equations arise due to the pressure difference when a fluid passes through a porous medium. So these terms exist only for electrode and catalyst zones in the domain. The source term, for low velocities of fluid, typical to those in fuel cells, is given by Darcy's law:

$$S_{px} = -\frac{\mu v_x}{\beta_x}, \quad z_1 \le z \le z_3 \quad (10)$$

$$S_{py} = -\frac{\mu v_y}{\beta_y}, \quad z_1 \le z \le z_3 \quad (11)$$

$$S_{pz} = -\frac{\mu v_z}{\beta_z}, \quad z_1 \le z \le z_3 \quad (12)$$

where μ is the viscosity of the fluid in the medium, and β is the permeability of the electrode material. Since the permeability of the medium was assumed to be isotropic, β_x, β_y and β_z each has a value of 10^{-12} m^2.

2.4. Boundary conditions

The boundary conditions were imposed for the model which was same for all the simulation cases. The operating temperature and pressure were set to 350 K and 2 atm, respectively. The mass-flow-inlet of the hydrogen reactant gas was kept constant at 2.5×10^{-7} kg/s. Also it was assumed that at the mass-flow-inlet the hydrogen reactant gas enters the gas flow-field channel normal to the cross-section of the channel.

2.5. Solution strategy

The model equations were solved using commercial computational fluid dynamics software Fluent® 6.0 with Gambit® as a preprocessor [4]. Control volume technique was used for solving the problem. The domain was divided into hexahedral volume elements with 20 nodes per element. The size of the hexahedron volume element chosen along with zone dimension in the problem domain is given in Table 1. The total number of volume elements in the flow-field distributor depends on the channel thickness and varies from case to case. In the gas distribution electrode and catalyst layer, the total number of volume elements was 102,400 and 25,600, respectively. A grid adaptation technique was used to obtain a solution which is independent of the dimensions of the chosen grid. The source terms were incorporated into Fluent® through the introduction of User Defined Functions (UDFs) code written in C language. The solution strategy is based on *simple* algorithm [4]. Momentum equations were solved for the velocity. This was followed by solving of equation of continuity, which updates the pressure and flow rate. Results were then checked for convergence. Since the density of the hydrogen gas varies from point to point, a technique similar to ideal gas technique was used for solving the model.

3. Results and discussion

Simulations were performed for different sets of channel dimensions. Three different parameters, viz. channel depth, channel height and land width between the channels were chosen for study. Each of the parameter was varied from 0.5 to 4.0 mm, resulting in total for six different dimensions

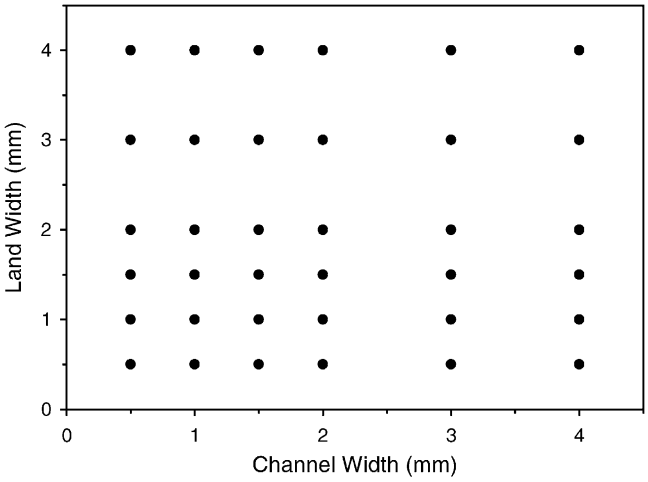

Fig. 3. Simulations cases corresponding to different channel width and land width at fixed channel depth.

cases (0.5, 1.0, 1.5 2.0, 3.0 and 4.0 mm). These cases are represented graphically in Fig. 3 for one depth. With all permutations and combinations amongst the parameters we have a total of $6 \times 6 \times 6 = 216$ cases.

We chose the hydrogen consumption at anode, as the parameter to judge the performance of the fuel cell. It may be noted that higher the hydrogen consumption at the anode better will be the fuel cell performance. Simulations corresponding to these 216 cases were done for different chosen values of λ. We choose four different values of λ corresponding to 5, 10, 15 and 20. The hydrogen consumption for each of these cases came out to be roughly 20, 42, 63 and 83 mass%, respectively. Considering the fact, that the practical fuel cell operates at high value of fuel consumption (like 80 mass%), we decided to choose the value of λ as 20 for our simulations. Further the simulations done at low values of λ like 5 or 10, showed little effect of changing the channel dimensions on hydrogen consumption. This was expected, since diffusion mass limitations of hydrogen in areas on ribs (land area) would be small at low reaction rates (low hydrogen consumption).

Fig. 4a–f shows the contour plots of consumption of hydrogen at anode as a function of channel width and land width. Each of the figures is plotted for constant channel depths ranging from 0.5 to 4.0 mm. As is clear in each of these figures, a region of maximum hydrogen consumption exists, corresponding to an optimum value for the channel width and land width. For example, in Fig. 4a, the region corresponding to channel depth of 1.5 mm and land width of 0.5 mm shows a maximum hydrogen consumption, and hence will perform better. Similar behavior was observed in other cases too. So we have a region of optimum dimensions of the channel width and land width. This is kind of an expected phenomenon, since the gases have to diffuse under electrode areas beneath the ribs. So in cases of large land width, diffusion mass limitations occur, and hence the net consumption of hydrogen decreases. Increasing the channel width results in decrease in the total length of the channels (or number of channels), and hence the pressure drop in the channels decreases, which lowers the performance. Second thing which can be noticed from these simulations results are that the hydrogen contours are more closely placed beyond the optimal point in increasing land width direction than in increasing channel width direction. This implies that increasing the land width has more sensitiveness than increasing the channel width on the hydrogen consumption at the anode. This is due to pronounced diffusion mass limitation of hydrogen beneath the ribs when land width is increased. The interesting phenomena in all these simulations results is that maxima for hydrogen consumption in all the cases occur near to the minimum land width (0.5 mm) which was chosen for the study. This makes us to believe that smaller land width will definitely improve upon the hydrogen consumption at the anode. The effect of channel depth on hydrogen consumption can be studied by comparing the Fig. 4a–f. We see that for case, when channel depth was 1.5 mm, maximum hydrogen consumption (84.8%) at anode takes place. On either sides, i.e. when the channel depth is decreased or increased beyond 1.5 mm, the consumption of hydrogen in the flow-field decreases. However, the decrease was more when channel depth was decreased. This is more clearly represented in Fig. 5 which shows the effect of change in channel depth with hydrogen consumption at anode at optimum channel width (1.5 mm) and land width (0.5 mm). So the established optimum dimensions from these simulations were channel width = 1.5 mm, land width = 0.5 mm and channel depth = 1.5 mm. These results were consistent with those observed by other researchers in their work. Watkins et al. [6] studied the optimal dimension for bipolar channels on cathode side of the fuel cell. They claimed the most preferred ranges to be 1.14–1.4 mm for channel width, 0.89–1.4 mm for land width and 1.02–2.04 mm for channel depth.

Based on the results, that the hydrogen consumption at anode increases as land width is decreased, we decided to study cases where land width can be reduced, close to a value of zero (0^+ mm). However, making such bipolar plates flow-field channels with very small land width ($\sim$0 mm) by machining or casting process is not practically feasible. Therefore, alternative methods must be looked at to fabricate such designs. One such method which can be employed is that of corrugated rolling process. However, this method is good only for metals/alloys systems. Keeping in mind that the currently used graphite bipolar plates suffer from some disadvantages (high machining cost, low mechanical properties, etc. [7,8]) and much of research is focused on use of metallic bipolar plates, we decide to study these systems.

Based on the foregoing discussion, we decided to use corrugated metallic bipolar plate for our simulation. The cross-section of the channel in these plates was triangular instead of the conventionally used rectangular cross-section in graphite bipolar plates. Before modeling for the triangular cross-section we wanted to quickly look, if such cross-section channels will perform better or at least comparable to that of square cross-section channels. So we decided to

study the pressure drop in channels for different cross-sections (rectangular, triangular and hemispherical), which would give an idea about the performance of the triangular or hemispherical shaped cross-sections in flow-field design of the bipolar plate.

The flow rate (q)–pressure drop (ΔP) relationships for some of the basic cross-section shaped channels are given in Eqs. (13)–(15). Each of the expressions is plotted in Fig. 6, for same channel width (1 mm).

Rectangular cross-section (square: $a = b = 1$ mm) [9]:

$$q = \frac{4ba^3}{3\mu} \times \frac{-\Delta P}{\Delta x}\left[1 - \frac{192}{\pi^5 b}\sum_{i=1,3,5,\ldots}^{\infty}\frac{\tanh(i\pi b/2a)}{i^5}\right] \quad (13)$$

Triangular cross-section (equilateral triangle: $a = 1$ mm) [9]:

$$q = \frac{\sqrt{3}a^4}{320\mu}\left(-\frac{\Delta P}{\Delta x}\right) \quad (14)$$

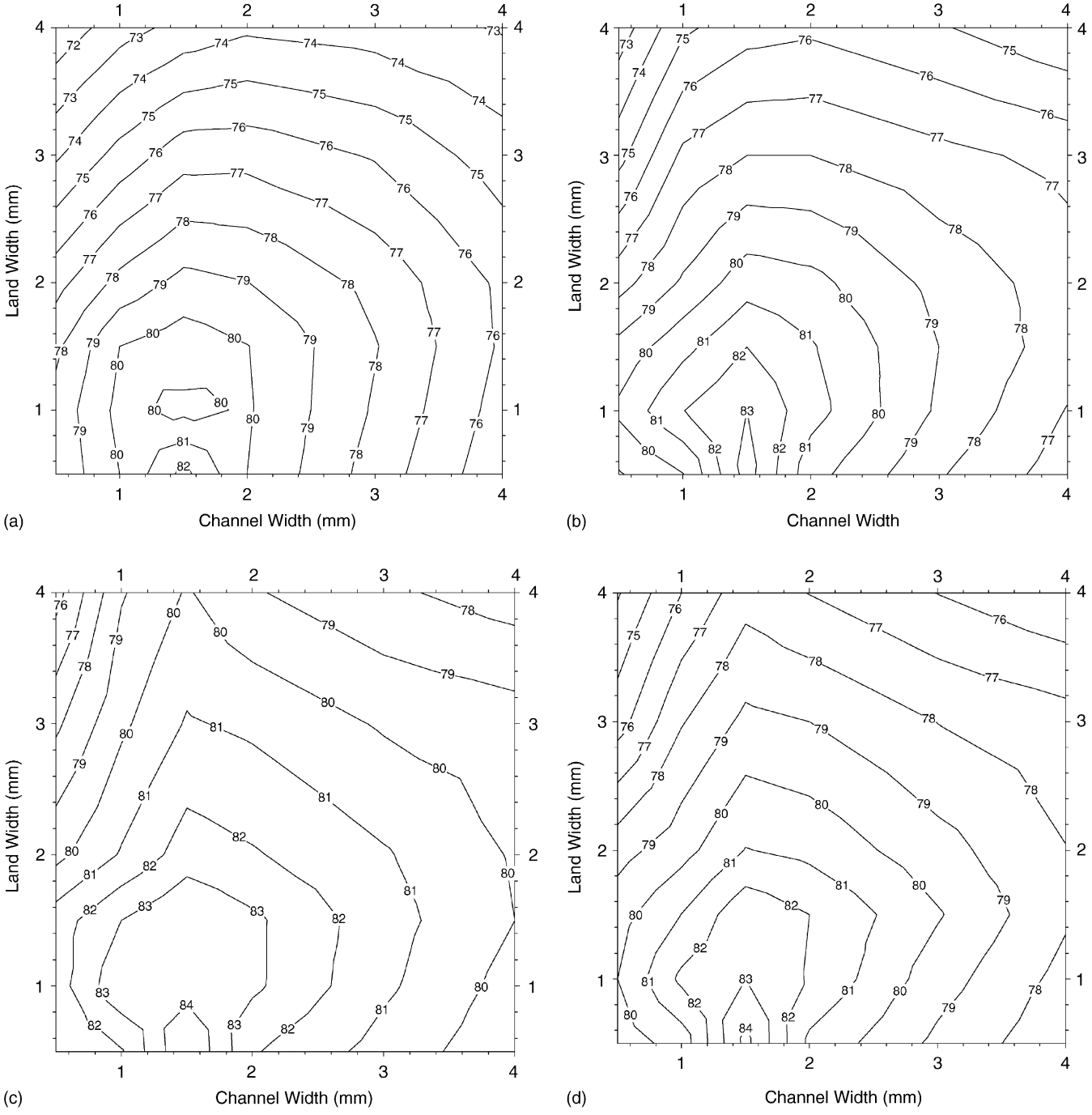

Fig. 4. Contour plots for the hydrogen consumption at anode as a function of channel width and land width for channel depth of: (a) 0.5 mm, (b) 1.0 mm, (c) 1.5 mm, (d) 2.0 mm, (e) 3.0 mm, and (f) 4.0 mm.

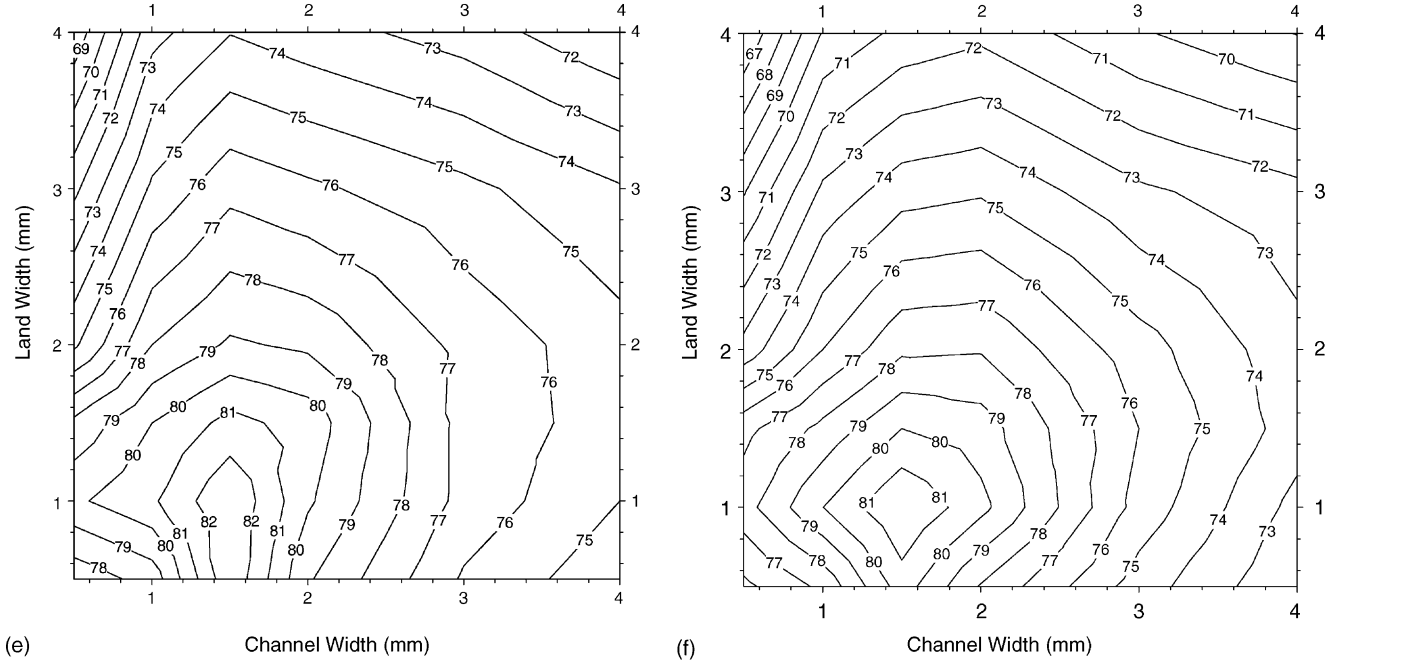

Fig. 4. (*Continued*).

Circular sector (hemisphere: $a = 0.5$ mm, $\alpha = \pi$ radians) [9]:

$$q = \frac{a^4}{4\mu}\left(-\frac{\Delta P}{\Delta x}\right)\left[\frac{\tan(\alpha)-\alpha}{4} - \frac{32\alpha^4}{\pi^5} \times \sum_{i=1,3,5,\ldots}^{\infty} \frac{1}{i(i+(2\alpha/\pi))^2(i-(2\alpha/\pi))}\right] \quad (15)$$

As can be seen from Fig. 6, hemispherical cross-section channels results in maximum pressure drop flowed by triangular cross-section. The pressure drop in these shaped cross-sections is around six to seven times higher at a gas flow rate of 20 cm^3/s, than that of rectangular cross-sectional channel, and hence will perform better in fuel cell. So we decided to model these cross-sections for the flow-field design using the Fluent® CFD tool. Using such channels serves our two purposes. Firstly we can achieve close to zero value for land width, and secondly, we can achieve higher pressure drop, both of which will provide enhanced fuel cell performance.

The simulations results for the triangular and hemispherical shaped cross-sections are represented in Fig. 7. These results are plotted for optimum channel dimensions which were obtained for rectangular shaped cross-section channels. For triangular cross-section these dimensions are: channel width = 1.5 mm, channel depth = 1.5 mm, and land width = 0^+ mm and for hemispherical cross-section:

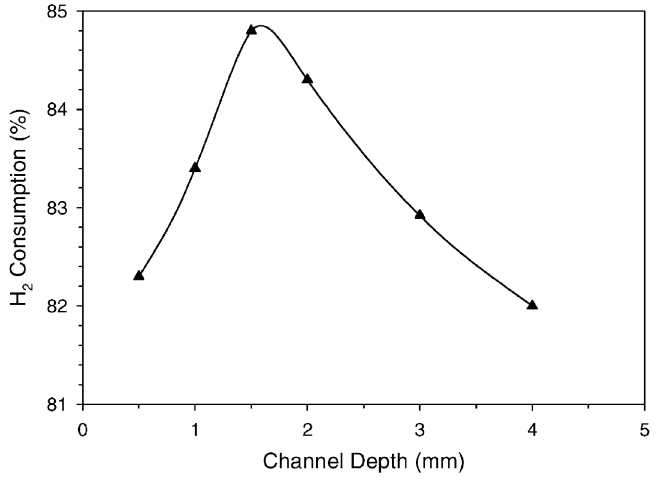

Fig. 5. Effect of channel depth on hydrogen consumption at the anode.

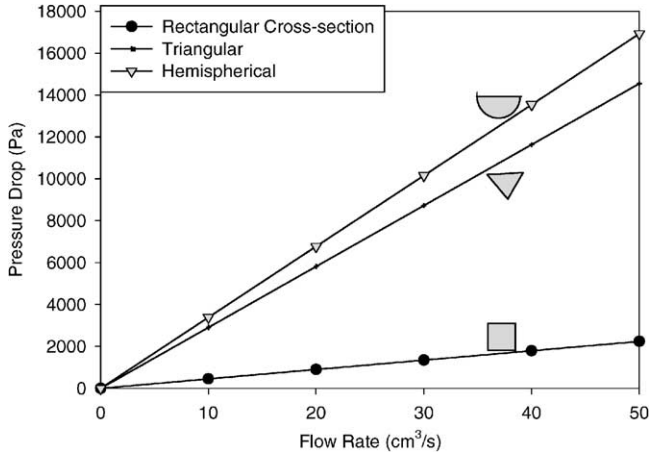

Fig. 6. Effect of channel shape on the pressure drop in the channels.

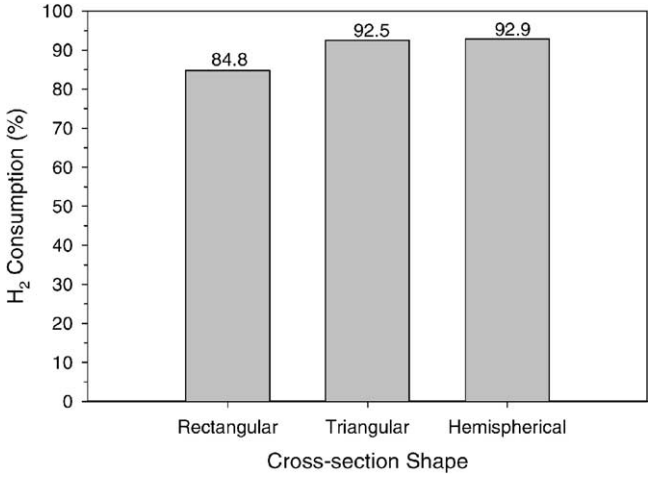

Fig. 7. Effect of channel cross-section on hydrogen consumption in the bipolar plate flow-field.

channel width = 1.5 mm, land width = 0^+ mm. It may be noted that in case of hemispherical cross-section, by choosing the channel width as 1.5 mm (diameter of hemisphere), the channel depth (radius of hemisphere) became 0.75 mm. The bar graph (Fig. 7) shows the hydrogen consumption at the anode for triangular and square cross-sections and compares these values to that for rectangular cross-section. The hydrogen consumption for the triangular shaped cross-section channels was 92.5% while that for hemispherical shaped cross-section channels was 92.9%. These values are approximately 9% more than that for rectangular shaped cross-section (84.8%). So it is clear that with use of cross-section other than rectangular shapes (like triangular and hemispherical) will enhance the hydrogen consumption at the anode, which in term will enhance the fuel cell performance.

4. Conclusions

A computational three-dimensional half-cell model for predicting the effect of different channels dimensions and shapes in the flow-field of the bipolar plate was developed. Simulations were performed using the commercial computation fluid dynamics software Fluent® 6.0. Simulations results for different channel dimensions showed that optimum values exist for channel width, land width and channel depths. It was found that for high fuel consumption (∼80%), which is more close to a practical case, the optimum channel width, land width and channel depth were close to values of 1.5, 0.5 and 1.5 mm, respectively. Also, it was found that decreasing the land width will increase the hydrogen consumption at the anode. Based on this, triangular and hemispherical cross-section shaped channels were studied. For these shapes, the land width is close to 0 mm. Simulation results for these shapes showed an increase in hydrogen consumption by 9% over the rectangular shaped cross-section. The use of such channels with proper dimensions will lead to increased hydrogen consumption at the anode, which in turn will lead to better fuel cell performance.

Acknowledgements

The authors are grateful for the support of this work by Center of Advanced Vehicle Technologies (CAVT) at The University of Alabama, which is funded by United States Department of Transport (US DOT), Grant No. DTFH61-91-X-00007.

References

[1] Fuel Cell Handbook, 5th ed. EG&G Services, Parsons Inc., US Department of Energy, Office of Fossil Energy, National Energy Technology Laboratory, West Virginia, 2000, pp. 1.1–1.37.
[2] Review of the Research Program of the Partnership for a New Generation of Vehicles (PNGV), Sixth Report, Report PNGV/2000, National Academy Press, Washington, DC, 2000.
[3] NECAR 4: The Alternative, Report Daimler Chrysler, Corporate Communications, Stuttgart, 1999.
[4] Fluent® 6.0 Users Guide Documentation, Fluent Inc., Lebanon, New Hampshire, 2001.
[5] E. Hontanon, M.J. Escudero, C. Bautista, P.L. Garcia-Ybarra, L. Daza, Optimisation of flow-field in polymer electrolyte membrane fuel cells using computational fluid dynamics technique, J. Power Sources 86 (2000) 363–368.
[6] D.S. Watkins, K.W. Dircks, D.G. Epp, Novel fuel cell fluid flow field plate, US Patent 4988583 (1991).
[7] A. Kumar, R.G. Reddy, PEM Fuel Cell Bipolar Plates—Material Selection, Design and Integration, in: P.R. Taylor (Ed.), Proceedings of the 2002 TMS Annual Meeting, TMS, Warrendale, PA, 2002, pp. 41–53.
[8] F. Barbir, J. Braun, J. Neutzler, Energy Partners Report 1999, Report Energy Partners, 1999.
[9] F.M. White, Viscous Fluid Flow, McGraw-Hill, New York, 1991, pp. 119–122.